Broadband Radio Spectral Observations of Solar Eclipse on 2008-08-01 and Implications on the Quiet Sun Atmospheric Model

Baolin Tan[1], Yihua Yan, Yin Zhang, Chengmin Tan, Jing Huang, Yuying Liu, Qijun Fu, ZhiJun Chen,Fei Liu, Linjie Chen and Guoshu Ji

Key Laboratory of Solar Activity, National Astronomical Observatories
Chinese Academy of Sciences, China

bltan@nao.cas.cn

Received July 15, 2009; accepted July 18, 2009; published online September 18, 2009
†Corresponding author (email: bltan@nao.cas.cn)

doi:10.1007/s11433-009-0230-y, published on Sci. China Ser. G, 2009, Vol.52, page 1765-1772

1. Introduction

Without the high-resolution solar radioheliograph, the solar radio eclipse observations may be the best way to investigate the spatial structure of the solar radio emission. During the minimum phase of solar cycle, the influence of the active regions is very weak, we may study the quiet solar coronal atmospheric model by means of the radio eclipse observations[1].

On August 1, 2008, a grand solar total eclipse could occurred on the regions of northern Europe and northwestern China. In Jiuquan of Gansu province, people could observe the whole course of eclipse happening. In Beijing, people could also watch the partial solar eclipse clearly. Around this event, the Sun was in a quiet phase between solar cycle 23 and 24. There was no solar flare, no corona mass ejection (CME), no sunspot, and no any active regions. The solar disk looked like a fairly clean plate. Such total eclipse might provide a god-given opportunity to test the quiet Sun atmospheric models by means of radio observations. During this solar eclipse, we made an extensive broadband spectral radio joint-observations at Jiuquan and Beijing Huairou. Section 2 introduces the observed instruments and the related data processing. Section 3 is a deduction of the quiet Sun atmospheric model from the above data. And some discussions and conclusions make up the final part of the paper.

2. Observations and Data Processing

The joint-observation included a solar total eclipse and partial eclipse observations. The solar total eclipse observations were carried out at Jiuquan with a broadband spectrometer (hereafter, EcBS/Jiuquan) in the frequency range of 2.00 – 5.60 GHz[2]. However, because of instrument problems, we only obtained a segment of valid data in the frequency of 3.60 – 5.60 GHz. The telescope was a newly updated instrument manufactured just before July of 2008 with an aperture of 2.40 m, not of very good performance. The status of the telescope tracking the Sun was recorded by a small CCD camera, connected to a small optical telescope and a computer. They were in-phase with the radio receiver by an GPS system. The axes of the CCD camera and the radio telescope were parallel to each other. The time cadence was about 10 pictures per second. Figure 1 presents the results of the CCD monitoring and the occulted information at three different times. The time cadence of the recorded radio data was 7.5 ms. This means that, in each

segment of 7.5 ms the receiver would do a whole scan in the frequency range of 2.0 – 5.60 GHz and recorded them, and it makes a recorded unit. Each recorded file includes 4 MB data in about 8000 recorded units. However, as a result of the missing and disordered data, each recorded file included actually about 6000 – 7000 valid recorded units. The time length in each recorded file was about 3.0 – 7.00 s with the averaged value about 5.59 s. As the magnitude of the fluctuation among the recorded units was very strong, we might integrate them into each recorded file. As for the frequency bandwidth, we might integrate them into 28 MHz at each channel. The solar radio partial eclipse observation is made by the Chinese solar broadband radiospectrometer (SBRS/Huairou) in Beijing Huairou in the valid frequency range of 2.60 – 3.80 GHz and 5.20 – 7.60 GHz[3,4]. The time cadence of the recorded data was integrated into 0.2 s, and the frequency bandwidth at each channel was 10 MHZ in the range of 2.60 – 3.80 GHz and 20 MHz in the range of 5.20 – 7.60 GHz. The performance of SBRS/Huairou was in good status.

As for the solar total eclipse at Jiuquan, the first optical contact was at $10^h16^m36.5^s$ UT with the solar photospheric radius 945.5 arcsecond and the lunar radius 978.1 arcsecond, and the totality began at $11^h13^m41.4^s$ UT and ended at $11^h15^m21.8$ UT. The maximum phase was at $11^h14^m31.7^s$ UT, the eclipse factor was 1.034477, the solar photospheric radius is 945.5 arcsecond, the lunar radius is 978.1 arcsecond, and the distance between the solar disk center and the lunar center was 12.95 arcsecond. The last contact was at $12^h08^m24.0^s$ UT with an altazimuth low to 4.4 degree. However, as the antenna could not follow the Sun's track after 11^h45^m UT, we could not get the radio observations after that time. As for the partial eclipse at Huairou, Beijing, the first optical contact was at $10^h16^m36.1^s$ UT with the solar photospheric radius 945.5 arcsecond and the lunar radius 977.7 arcsecond. The maximum phase was at $11^h09^m23.2^s$ UT with an eclipse factor of 0.910905, and with the solar photospheric radius 945.5 arcsecond and the lunar radius 974.7 arcsecond, and the distance between the solar disk center and the lunar center 190.04 arcsecond. The last contact was at $11^h59^m11.3^s$ UT, much after the sunset (The corresponding sunset time at Huairou Station was about 11^h28^m UT). So, we could not get the observation data about the partial eclipse after the maximum phase.

The calibration and data processing method follow the Ref.[5 and 6]. Before and after the period of eclipse, the calibrating observations are made and and the emission measure of the sky background along the Sun's routine corresponding to the solar eclipse is taken. As the Sun was in its quiet phase, the polarization of radio emission was very weak. It is unimportant to differentiate the right circular polarized emission (RCP) and the left circular polarized emission (LCP). This work adopted the total emission intensity (RCP+LCP). As the instrument of SBRS/Huairou was aging, while the telescope of EcBS/Jiuquan was a new instrument, the signal fluctuation was fairly strong. We make a broad averaging with the data. So our result is smoothed one (as for the data of EcBS/Jiuquan, we make averaging in each recorded file, so the integrated time is about 3 – 7 s with the mean value of 5.59 s; as for the data of SBRS/Huairou, we make averaging in each segment of 3.2 s). At the same time, as the period of the eclipse was very close to the sunset, it's hard to remove the disturbances coming from the subaerial factors.

In this work we mainly focus on the processes occurring at around the first radio contact of the Moon's limb to the solar disk. We select three segments of frequency to form a successive broadband observations with frequency of 2.60 – 7.60 GHz. The first (2.60 – 3.80 GHz) and third (5.20 – 7.60 GHz) segment were obtained at SBRS/Huairou, while the second segment (3.80 – 5.60 GHz) was observed by EcBS/Jiuquan. Figure 1 shows the solar radio eclipse curves which includes the Jiuquan total eclipse (left and right panels) and the Huairou partial eclipse (middle panel). The region marked with **M** between two vertical solid lines in the left panel is most likely to be a disturbance from some unknown terrestrial factor. Figure 2 presents the solar radio eclipse slope curves one by one with Figure 1. The horizontal dashed lines in the left panels

indicate the zero level of the slopes. The vertical solid lines in the left and right panels indicate the time of the first optical contact and the maximum phase of the partial eclipse, respectively. While the vertical solid lines in the middle panels indicate the time of the first optical contact and the totality phase of the total eclipse, respectively. All of the solid thick curves in Figure 1 and Figure 2 are smoothed in brand slide windows which reflect the main tendency of the solar radio eclipse curves and the radio eclipse slope curves.

3. Results and some Implications about Quiet Sun Atmospheric Model

3.1. Results

Generally, from the solar radio eclipse curves we can get the time of the first radio contact and determinate the solar radio radii[7]. However, from Figure 1 we can find that the fluctuation of the radio eclipse curves is fairly strong. It is not easy to determine the exact time of the first radio contact of the eclipse just from the solar radio eclipse curves (dashed lines in Figure 1), even if from the smoothed curves (solid thick lines in Figure 1). Here, we apply the solar radio eclipse slope curves (Figure 2) to obtain the relatively exact time of the first solar radio contact. The following is the basic working principle: the telescope antenna is always pointed to the center of the solar disk, before the first radio contact. The receiver gets the whole solar radio emission, and the slope curves should be approximated to a horizontal line around zero; from the beginning of the eclipse (first contact), when the receiver gets less and less solar radio emission with the increasing of the solar disk occulted by the Moon, the slope curve will become negative. Then we may define the intersection point between the smoothed slope curve and the zero horizontal line as the time of the first solar radio contact of the eclipse. The arrows in Figure 2 indicate the time of the first solar radio contact of the eclipse at each frequency, with corresponding values (t_{ra}) listed in Table 1.

Based on t_{ra}, we can calculate the solar radio radii (r):

$$r = \frac{t_1 - t_{ra}}{t_\odot} + 1. \tag{1}$$

Here, t_1 is the time of the first optical contact of the eclipse, as for the solar total eclipse at Jiuquan, t_1=$10^h16^m36.5^s$ UT; as for the partial eclipse at Huairou, Beijing, t_1=$10^h16^m36.1^s$ UT. $t_\odot$ indicates the time when the Moon's limb moves for a distance of a solar photospheric radius $R_\odot$, and can be calculated from the following equation:

$$t_\odot = \frac{t_{max} - t_1}{\frac{\sqrt{(R_\odot + r_{mo})^2 - h^2}}{R_\odot}} \tag{2}$$

t_{max} stands for the time of the maximum phase of the eclipse, r_{mo} for the lunar radius at the time of the first optical contact, and h for the distance between the solar disk center and the lunar center at the maximum phase. As for the solar total eclipse at Jiuquan, t_{max}=$11^h14^m31.7^s$ UT, h = 12.95 arcsecond, r_{mo} = 978.1 arcsecond, then $t_\odot$ = 1705.18 s; as for the partial eclipse at SBRS/Huairou t_{max}=$11^h09^m23.2^s$ UT, h = 190.04 arcsecond, r_{mo} = 977.7 arcsecond, then $t_\odot$ = 1564.70 s. Here, we assume that the relative velocity of the Moon versus the Sun is uniform.

The observational solar radio radii and the emission flux before the time of the first radio contact of the eclipse are also listed in Table 1. Figure 3 presents the distribution of the solar radio radii with frequencies.

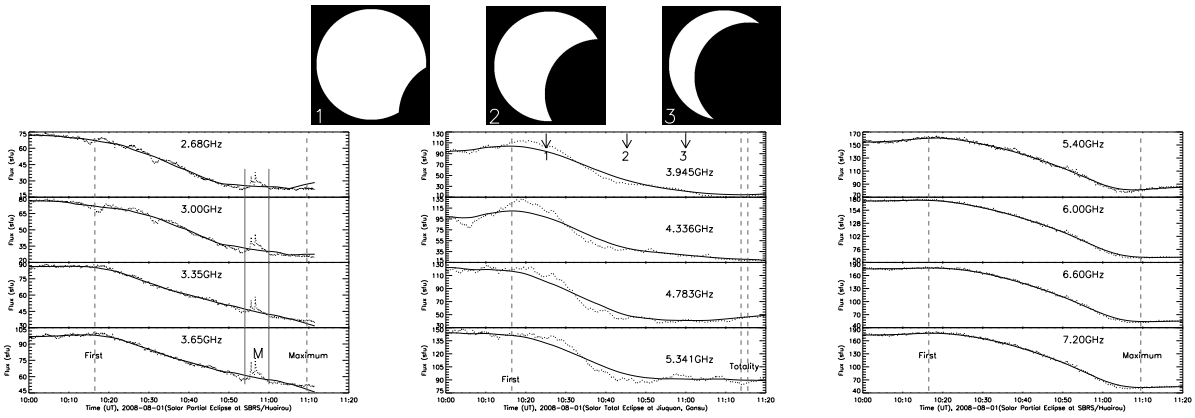

Fig. 1.— Solar radio eclipse curves of August 1, 2008. Left: 2.60 – 3.80 GHz, partial eclipse, SBRS/Huairou, Beijing, the region marked with **M** between two vertical solid lines is most likely to be a disturbance from some unknown terrestrial factor; Middle: 3.80 – 5.20 GHz, total eclipse, Jiuquan, Gansu, the upper small figures are CCD monitoring observations, from left to right (marked as 1, 2, 3 corresponding to the arrows with the same numbers), the time is at 10:25 UT, 10:45 UT, and 11:00 UT, respectively; Right: 5.20 – 7.60 GHz, partial eclipse, SBRS/Huairou, Beijing.

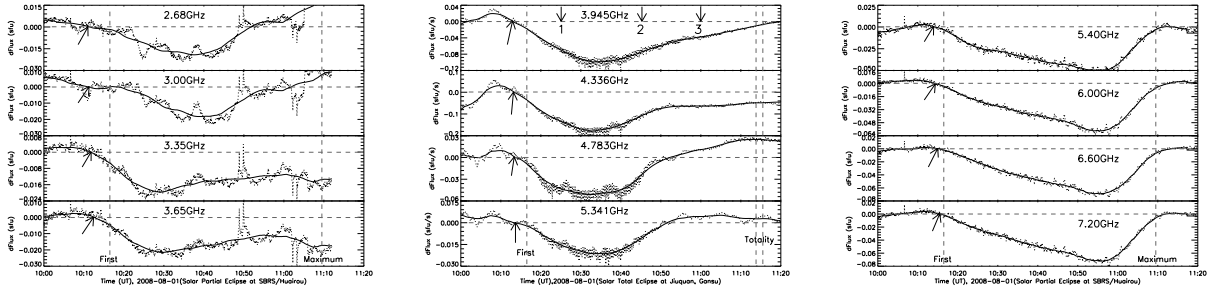

Fig. 2.— Solar radio eclipse slope curves of August 1, 2008. Left: 2.60 – 3.80 GHz, partial eclipse, SBRS/Huairou, Beijing; Middle: 3.80 – 5.20 GHz, total eclipse, Jiuquan, Gansu; Right: 5.20 – 7.60 GHz, partial eclipse, SBRS/Huairou, Beijing. The arrows below the curves indicate locations of the first solar radio contact of the eclipse, and the vertical arrows with number 1, 2, 3 indicate three instants as in Figure 1.

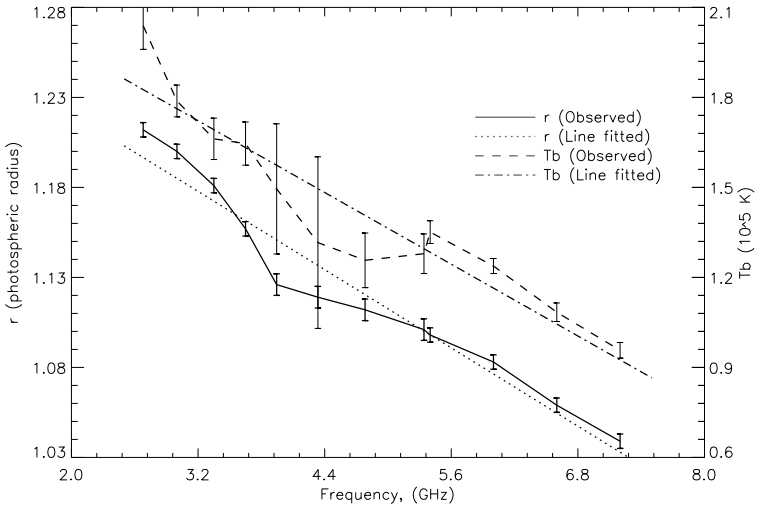

Fig. 3.— Results of the solar radio radii (r, in unit of solar photospheric radius) and the bright temperature (T_b) in the frequency of 2.0 – 7.60 GHz observed in the solar eclipse of 2008-08-01 at EcBS/Jiuquan and SBRS/Huairou.

Table 1: The list of VLP, LPP and SPP occurred in the flare event on 2006-12-13. Here the frequency drifting rate is the averages values in the unit of MHz/s, and the bandwidth is also in MHz, both of duration and period are in unit of second.

f(GHz)	t_{ra} (UT)	$r(\mathrm{R}_\odot)$	Flx (sfu)	$T_b(10^5K)$	$n_e(10^9cm^{-3})$	Instrument
2.680	$10^h11^m04^s$	1.212 ± 0.002	71.5 ± 2.72	2.039 ± 0.079	2.06 ± 0.05	SBRS/Huairou
3.000	$10^h11^m22^s$	1.200 ± 0.002	77.0 ± 2.32	1.788 ± 0.053	2.11 ± 0.04	SBRS/Huairou
3.350	$10^h11^m53^s$	1.181 ± 0.002	86.5 ± 3.55	1.662 ± 0.069	2.25 ± 0.05	SBRS/Huairou
3.650	$10^h12^m30^s$	1.157 ± 0.002	97.5 ± 4.24	1.646 ± 0.072	2.43 ± 0.06	SBRS/Huairou
3.945	$10^h12^m01^s$	1.126 ± 0.003	98.0 ± 13.94	1.495 ± 0.217	2.46 ± 0.20	EcBS/Jiuquan
4.336	$10^h12^m13^s$	1.119 ± 0.003	103.0 ± 22.38	1.316 ± 0.286	2.49 ± 0.31	EcBS/Jiuquan
4.783	$10^h13^m25^s$	1.112 ± 0.003	118.0 ± 8.50	1.257 ± 0.091	2.67 ± 0.12	EcBS/Jiuquan
5.341	$10^h13^m44^s$	1.101 ± 0.003	147.0 ± 7.45	1.279 ± 0.066	3.02 ± 0.09	EcBS/Jiuquan
5.400	$10^h14^m02^s$	1.098 ± 0.002	158.0 ± 4.36	1.351 ± 0.038	3.18 ± 0.05	SBRS/Huairou
6.000	$10^h14^m27^s$	1.083 ± 0.002	173.6 ± 3.33	1.238 ± 0.025	3.33 ± 0.04	SBRS/Huairou
6.600	$10^h15^m03^s$	1.059 ± 0.002	176.2 ± 5.32	1.084 ± 0.031	3.35 ± 0.06	SBRS/Huairou
7.200	$10^h15^m34^s$	1.039 ± 0.002	178.0 ± 4.95	0.957 ± 0.026	3.37 ± 0.06	SBRS/Huairou

From this figure we find that the curve is most likely to be a beeline. We operate a best linear fit and get a linear function:

$$r = 1.29370 - 0.036224f \tag{3}$$

Here, the unit of solar radio radius r is in solar photospheric radius ($R_\odot$), and the frequency f is in GHz.

Then, we calculate the bright temperature of the radio quiet Sun at each frequency:

$$T_b = \frac{c^2 D^2 Flx}{k_B f^2 (rR_\odot)^2} = 3.009 \times 10^{22} \frac{Flx}{f^2 r^2} \tag{4}$$

Here, Flx is unit in sfu, and f is in Hz. D is the averaged distance from the Sun to Earth. The bright temperature at each frequency is also listed in Table 1, and plotted in Figure 3.

As mentioned in section 1, the Sun was in its quiet phase. We may simply assume that: (1) the microwave emission is mainly originated from the bremsstrahlung mechanism of thermal plasma in which the electron density is approximated to that of ions ($n_e \approx n_i$); (2) the solar atmosphere is spherically symmetrical; (3) the absorption effects can be ignored. Then we can make out the estimation of the electron plasma density:

$$n_e \simeq 1.2416 \times 10^{12} \frac{Flx^{1/2} T_b^{1/4}}{r(M \triangle l)^{1/2}}, (cm^{-3}) \tag{5}$$

Here, $M = 19.38 + \frac{3}{2} ln T_b - ln f$, and $\triangle l$ is the characteristic length of the emitting medium along the line of sight. Simply, we make $\triangle l \sim 5000$ km for all frequencies. The result of n_e is listed in Table 1, and plotted in Figure 4.

From these results we find that the bright temperature of the coronal plasma is in the range of 9.57×10^4 – 2.04×10^5 K, and the plasma density is in the range of 2.05×10^9 – $3.37 \times 10^9 cm^{-3}$ at the height of 2.7×10^4 – 1.5×10^5 km ($r = 1.039 - 1.212 R_\odot$) above the solar photosphere.

3.2. Error Analysis

Generally, the fluctuation of the radio emission during the eclipse was fairly strong with obvious errors, so was the case with Huairou and Jiuquan observations, because SBRS was old and ECBS was new. We make a broad averaging with the data. The error of solar radio radii (r), bright temperature (T_b), and electron plasma density (n_e) can be expressed as: $\triangle r = \pm \frac{\triangle t_{ra}}{t_\odot}$, $\triangle T_b = \pm T_b (\frac{\triangle Flx}{Flx} + \frac{2\triangle f}{f} + \frac{2\triangle r}{r})$, and $\triangle n_e = \pm n_e (\frac{\triangle r}{r} + \frac{\triangle Flx}{2Flx} + \frac{\sqrt{M}-3}{4M} \frac{\triangle T_b}{T_b})$, respectively. We make 3 times of standard deviation as the error of emission flux, $\triangle Flx = 3\sigma_{Flx}$. As for the data of EcBS/Jiuquan, we make averaging in each recorded file, so the integrated time is about 3 – 7 s with the mean value of 5.59 s, so $\triangle t_{ra} = 5.59$s, $\triangle r = \pm 0.003 R_\odot$; $\triangle f = 28$ MHz. As for the data of SBRS/Huairou, we make averaging in each segment of 3.2 s, $\triangle t_{ra} = 3.2$ s, $\triangle r = \pm 0.002 R_\odot$; $\triangle f = 10$ MHz in frequency of 2.60–3.80 GHz, and 20 MHz in 5.20–7.60 GHz. Then $\triangle T_b$, and $\triangle n_e$ can be made out (listed in Table 1).

These analyses show that the error level of EcBS/Jiuquan is higher than that of SBRS/Huairou.

3.3. Implications about Quiet Sun Atmospheric Model

The solar radio radius is an important quantity in studying the solar atmospheric model since the height above the photosphere at which the radio emission originates at different frequencies defines the plasma density distribution. With these results, we can deduce the seimiempirical solar atmospheric model. The optical and millimeter radio observations can present the solar photospheric and chromospheric models[8,9,10,11]. Fontenla, Balasubramniam, and Harder gave a semiempirical model of the quiet Sun low chromosphere at moderate resolution[12]. The cm and dm wavelength radio observations will provide the information of the solar coronal atmospheric model. From the above results, we know that the emission region of the 2.60-7.60 GHz radio emission must be located in the corona. As most of the eruptive processes always occur in these region, a perfect coronal model, especially the semiempirical models from the observations, is very important for understanding physical processes in the Sun. During the quiet phase of solar cycle, the magnetic field was very weak and fairly uniform. There was almost no magnetic active regions. It is easier to set up a fairly perfect atmospheric model of the quiet Sun.

Figure 4 presents the comparison between the observed result of coronal density and the classic Baumbach-Allen's model. Baumbach-Allen's model[13] can be expressed as:

$$n_e = m \times 10^8 (\frac{1.55}{r^6} + \frac{2.99}{r^{16}}), (cm^{-3}) \tag{6}$$

Here m is a given multiple. The solid line stands for the observed result. The dashed lines are Allen's models with m times. Here m is in the range of 12 – 32. However, from this figure we find that the curves of Baumbach-Allen's model are too steep to fit the observed results. We make a best-fit curve, the dashed-dotted line in Figure 4 is a best-fitted model which can be expressed as follows:

$$n_e \simeq 1.42 \times 10^9 (\frac{1}{r^2} + \frac{1.93}{r^5}), (cm^{-3}) \tag{7}$$

Based on the comparison between equations (6) and (7), we find that coronal plasma density is more likely to be associated with the low power of height (r) than that of the classic model.

4. Discussions and Conclusions

In this study work, we analyze the joint-observations of radio broadband spectral emissions during the solar eclipse on August 1, 2008 at Jiuquan (total eclipse, observed in the frequency of 2.00 – 5.60 GHz) and Huairou (partial eclipse, observed in the frequency of 2.60 – 3.80 GHz and 5.20 – 7.60 GHz). Using these telescopes, we can assemble a successive series of broadband spectrum with frequency of 2.60 – 7.60 GHz to observe the solar eclipse synchronously. With these analyses, we obtain a semiempirical quiet Sun coronal model (equation (7)) which indicates that the distribution of solar coronal plasma density in respect to the height is not so steep as the classic model, corresponding to the height of 2.7×10^4 – 1.5×10^5 km ($r = 1.039 - 1.212 R_\odot$) above the solar photosphere, and the bright temperature is in the range of $9.57 \times 10^4 - 2.04 \times 10^5$ K. This is consistent with the result of Ref [14].

However, our results are obtained from the range of 2.60 – 7.60 GHz, and only valid in the limited space of $r = 1.039 - 1.212 R_\odot$. It is necessary to enlarge the observing frequency range in the future observations. Additionally, the height angle of the eclipse of August 1, 2008 was very small. When the eclipse occurred,

the line-of-sight was fairly close to the ground, with many disturbances coming from the subaerial factors. The telescope of EcBS/Jiuquan, a new instrument, needs to be improved in many aspects. Fortunately, a more significant solar total eclipse will occur on July 22, 2009 in a more extended area along the Changjiang River, during 8-11 o'clock in the morning, and the height angle is very high. The observational condition is very good. We will make more detailed observations to get the further supports for our semiempirical model.

The authors would like to thank the anonymous referee for helpful and important comments. They also thank associate professor Cheng Zhuo from Purple Mountain Observatory of CAS (Nanjing) for the important data of the optical solar eclipse tracks of August 1, 2008. This work was supported by the CAS-NSFC Key Project (Grant No.10778605), the National Science Foundation of China (Grant Nos.10733020, 10843002, 10873021), and the MOST (Grant No.2006CB806301).

REFERENCES

Gary D.E. & Zirin H., Microwave structure of the quiet Sun. Astrophys J, 1988, 329:991-1001

Liu F., Chen L.J., Yan Y.H., Chen Z.J., & Ji G.S., A broadband digital receiver for solar eclipse radio observation. Sci China Ser G, 2009, submitted

Fu Q.J., Qin Z.H., Ji H.R., Pei L.B., A Broadband Spectrometer for Decimeter and Microwave Radio Bursts. Sol Phys, 1995, 160: 97

Ji H.R., Fu Q.J., Liu Y.Y., et al, A Solar Radio Spectrometer at 5.2-7.6 GHz. Sol Phys, 2003: 359

Yan Y.H., Tan C.M., Xu L., et al, Nonlinear calibration and data processing of the solar radio burst, Sci China Ser A, 2002, 45 Supp., 89

Zhou S.R., Radio Observation and pre-processing of the data for the solar eclipse, Publ Purple Mountain Obs, 1998, 17(4):1-7.

Swanson P.N., The radio radius of the Sun at millimeter and centimeter wavelengths, Sol Phys, 1973, 32: 77-80

Foukal P. Solar Astrophysics. John Wiley and Sons, Inc., 1980.

Allen C.W. Astrophysical Quantities, Athlone Press, London: 1973.

Piddungton J.H. A model of the quiet solar atmosphere. Sol Phys, 1972, 27: 402–419.

Furst E. The quiet Sun at cm and mm wavelength. IAU Symposium, 1980, 86: 25–39.

Fontenla J.M., Balasubramniam K.S., & Harder J. Semiempirical models of the solar atmosphere. II. The quiet-Sun low chromosphere at moderate resolution, Astrophys J, 2007, 667: 1243–1257.

Smerd S.F. Radio-frequency radiation from the quiet Sun, Australian J Sci Res A, 1950, 3: 34–59.

Subramanian K. R. Brightness temperature and size of the quiet Sun at 34.5 MHz, Astron Astrophys, 2004, 426: 329–331.

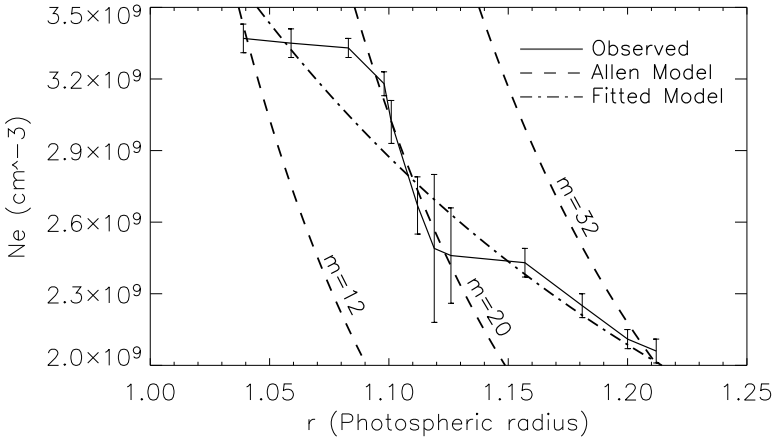

Fig. 4.— A Comparison between the observed result of coronal density and the Allen's model. The solid line represents the observed result. The dashed lines are Allen's models with m times. The dashed-dotted line is a best-fitted model expressed in Equation (6).